# Large signal periodic time-domain circuit simulation

K.R. Whight

*Indexing terms: Time-domains, Signal effects, Simulation*

**Abstract:** A novel time-domain algorithm has been applied in the field of circuit analysis to model large signal effects under periodic excitation. Conventionally, the need to integrate out initial transients over many cycles had effectively made time-domain simulation impractical. The new algorithm, however, neatly avoids this problem, yielding the periodic steady state directly by simulating over just one cycle. A prototype simulator has been written that implements the algorithm within a circuit context, and it has been used in a preliminary study of large signal harmonic effects in both driven and autonomous circuits. In particular, the following circuits are analysed: a single-stage transistor amplifier, a varicap tuner, a full wave rectifier and a Colpitts oscillator. The nonlinear effect of jump resonance is observed in the varicap tuner circuit. An extension of the basic algorithm beyond harmonic analysis into the realms of mixers and other possibly noncommensurate frequency circuits is proposed. Possibilities regarding mixed-mode circuit/device simulation are also discussed.

## 1 Introduction

Large signal periodic effects are an important class of problem that in the past have not been amenable to direct time-domain simulation. Transient time-domain simulation, although easy to perform for a circuit with any number of strongly nonlinear elements, suffers from the fact that the system being modelled may have time constants that are large compared to the fundamental excitation frequency. Thus many cycles may need to be integrated to overcome the effect of initial transients and to arrive at the final periodic steady state.

To avoid the problem of initial transients the author proposed a novel approach, within the field of semiconductor device modelling, which was implemented in the TESSA simulator [1]. This approach requires the system equations to be recast in a spacetime form, as it considers the time axis effectively to be additional dimension to which periodic boundary conditions are applied, i.e. periodicity is forced by the simulation mesh. In the circuit context this requires, in its simplest form, that the circuit nodes be automatically repeated on timeplanes. Each node on each timeplane is distinct and has a unique voltage variable associated with it. Each timeplane has an associated fundamental phase, but there are no nodal phase variables. Taking a spacetime viewpoint, the simulation mesh has a cylindrical topology with time running around the circumference of the cylinder, the distance around the cylinder being equal to the fundamental period. A more general description of the underlying method as applied to semiconductor device modelling is given in the TESSA paper [1].

The problem now becomes that of relating the current flowing between spatial node neighbours, i.e. on the same timeplane and connected by a circuit element to the voltages on relevant spacetime nodes. Once this has been achieved a matrix equation can be constructed, by applying Kirchoff's current conservation law at each spacetime node, in which the unknowns are all the spacetime nodel voltages. This process results in $n$ equations in the $n$ unknowns, which, on solution, yields directly the periodic steady state of the system.

The above method has been implemented in a prototype large signal circuit simulator (LARGESS) and the program has been used in this preliminary study of large signal effects in both driven and autonomous circuits. The circuits studied include a simple single-stage amplifier, a varicap tuner circuit, a full wave rectifier and a Colpitts oscillator. The results of these simulations are reported following a more detailed description of how circuit elements are treated in the method and an illustration of the matrix assembly process, using as an example a simple linear LCR series resonant circuit.

## 2 Spacetime formulation of circuit equations

To implement the proposed algorithm the current flowing through any circuit element at a given instant needs to be related to relevant spacetime nodal potentials. There are three distinct types of time dependence within current/voltage relationships that need to be considered, namely, those that have no time dependence (archetype: a resistor), those that have a time dependence that is a first-order differential of voltage (capacitor), and those that depend on an integral of voltage over time (inductor).

### 2.1 Resistor

From the definition of resistance we have

$$V = IR \tag{1}$$

from which the current flowing from node $i$ to node $j$ on timeplane 0 connected by a resistor of value $R$ is

$$I_{ij} = \frac{V_j^0 - V_i^0}{R} \tag{2}$$



Paper 1244G (E10), first received 1st October 1993 and in revised form 29th March 1994

The author is with the Philips Research Laboratories, Cross Oak Lane, Redhill, Surrey RH1 5HA, United Kingdom

### 2.2 Capacitor

The definition of capacitative current is

$$I = C\frac{dV}{dt} \tag{3}$$

Taking a first-order approximation of the time derivative we may write the current flowing from node $i$ to node $j$ on timeplane 0 through a capacitance of value $C$ as:

$$I_{ij} = C\frac{(V_j^0 - V_i^0 - V_j^- + V_i^-)}{\Delta t} \tag{4}$$

where the $^-$ superscript refers to the relevant equivalent node on the previous timeplane.

### 2.3 Inductor

The definition of inductive current is

$$I = \int \frac{V}{L}\,dt + i \tag{5}$$

where the integral represents the change in current flowing through the inductor, of inductance $L$, occurring during the time step $dt$ and $i$ is the constant of integration. The constant of integration may be obtained by associating a small 'sense resistor' in series with the inductor. Again to first-order only, we may write the current flowing from node $i$ to node $j$ on timeplane 0 as

$$I_{ij} = \frac{(V_j^- - V_i^-)\,\Delta t}{L} + \frac{V_k^- - V_l^-}{R} \tag{6}$$

where $k$ and $l$ are the nodes to which the sense resistor, of value $R$, is connected. The direction of current through the sense resistor needs to correspond to the direction through the inductor, and all the current flowing through the inductor must also flow through the resistor. It is not absolutely necessary to employ a sense resistor but it makes the matrix assembly process easier and, as all real inductances have series resistance, it is not considered to be an unreasonable requirement.

### 2.4 Example circuit equations for an LCR series resonant circuit

To illustrate the matrix assembly process a linear series resonant circuit will be considered (Fig. 1). In this Figure

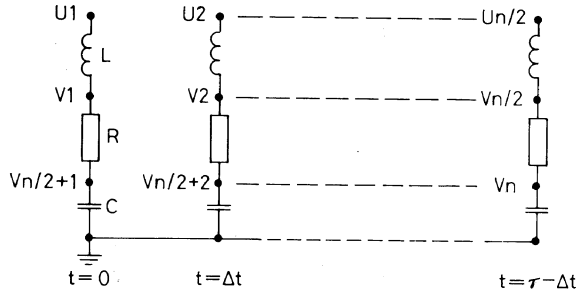


**Fig. 1** *Spacetime view of series resonant LCR circuit*

the circuit is seen to be repeated on timeplanes; however, the cylinder (of period $\tau$) has been cut at $t = 0$ and its surface laid flat. There are a total of $n$ free nodes at which the potentials ($V_i$ for $i = 1, 2, \ldots, n$) satisfying the circuit equations and boundary conditions are to be calculated simultaneously. There are also $n$ Dirichlet boundary condition nodes, of which $n/2$ are earthed, the remaining ones being at given fixed potentials $U_1, U_2, \ldots, U_{n/2}$. Note that the periodic temporal boundary condition implies that nodes on timeplane $t = \tau - \Delta t$ are to be considered as in the immediate past of nodes on timeplane $t = 0$. Also note that the resistor already present in the circuit will be used as the inductor's sense resistor, as all the current that passes through the inductor at any instant also passes through this resistor.

The matrix assembly process will be illustrated by writing down the equations necessary to satisfy Kirchoff's current conservation law at nodes 1 and $n/2 + 1$, the equations for the remaining nodes being similar to one or other of these.

*Node 1:* From eqns. 2 and 6 we may write

$$\left\{\frac{(U_{n/2} - V_{n/2})\,\Delta t}{L} + \frac{V_{n/2} - V_n}{R}\right\} + \frac{V_{n/2+1} - V_1}{R} = 0 \tag{7}$$

where the first term represents the inductive current out of the node and the second term the resistive current.

*Node $n/2 + 1$:* From eqns. 2 and 4 we may write

$$\frac{V_1 - V_{n/2+1}}{R} + \frac{C(V_n - V_{n/2+1})}{\Delta t} = 0 \tag{8}$$

where the first term represents the resistive current flowing from node $n/2 + 1$ and the second term is the capacitative current. Note that in this second term only two variables appear, as the other relevant nodes, required by eqn. 4, are in this case earthed Dirichlet nodes, i.e. at zero potential.

The above process, when continued for the remaining free nodes, results in a system of $n$ equations in the $n$ free nodal potentials which, being linear, is directly soluble for the periodic steady state. For nonlinear elements equations may be written down as above. However, the necessary Newton linearisation process would generate additional terms in the matrix when differentiating the nonlinear functions $L$, $C$ or $R$ with respect to the free nodal potentials.

## 3 LARGESS simulations: driven circuits

The circuit simulator LARGESS is written in C and uses data structures similar to those reported for TESSA [1]; the linear algebra routines are also similar, i.e. LU decomposition without pivoting. The direct solver option is used exclusively in this work and a Newton linearisation method is used to solve the nonlinear circuit equations. The program is currently restricted in the type of circuit element, e.g. only an Ebers–Moll transistor model is available, but it is capable of general topologies. The spatial circuit layout is described using a simple input language. A rudimentary postprocessing routine has been written that allows the output of either raw data, as a function of phase, or numerical Fourier analysis data, both in a form suitable for plotting. All simulations were performed on an Apollo DN10000 machine working at approximately 2.5 MFLOPS, i.e. unvectorised code.

### 3.1 Single-stage transistor amplifier

As a first example of the use of LARGESS the simple single-stage transistor amplifier circuit shown in Fig. 2 was simulated with an input sinusoid of 5 V at 10 kHz and a 10 V DC supply. An Ebers–Moll transistor model was used with diode characteristics given by

$$I = I_s(e^{qv/kt} - 1) \quad \text{for } -1 < v < 0.5\text{ V} \tag{9}$$

where $I_s = 1.0 \times 10^{-6}$ amp. Outside the above voltage range the characteristic was linearly extrapolated with

continuous first-order derivatives. The gains of the model's current-controlled current generators were $\alpha_f = 0.99$ and $\alpha_r = 0.5$. In Fig. 3 the output voltage at node 6

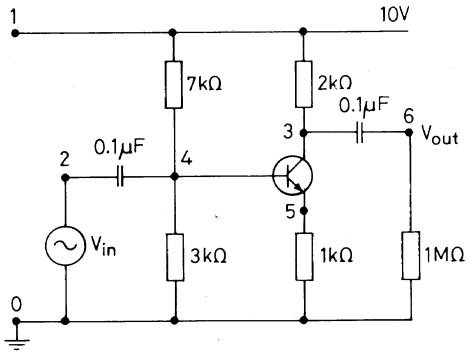


**Fig. 2** *Simulated amplifier circuit*

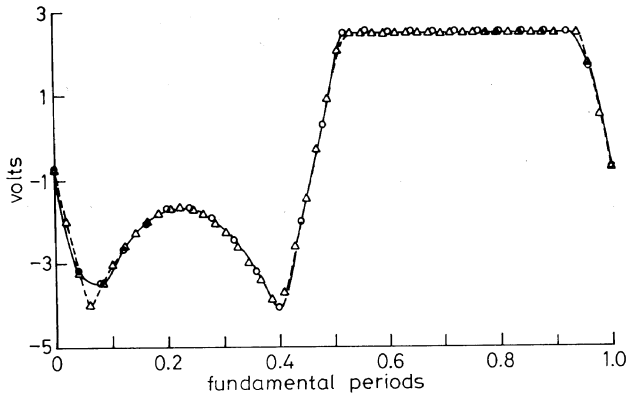


**Fig. 3** *Amplifier output waveform*
—○— 25 timeplanes
—△— 49 timeplanes

is shown as a function of time using 25 and 49 equispaced timeplanes spanning the 10 kHz period, the simulation CPU time was 5 s (25 timeplanes). It can be seen that the output is similar on both meshes, and severely distorted. The first (negative voltage) half period has a 'bite' out of it caused by the collector–base junction becoming forward biased. The latter half period exhibits clipping caused by the emitter–base junction becoming reverse biased.

Conventional transient simulation tends towards the waveform shown in Fig. 3, but takes in excess of 15 min CPU time, i.e. although the general waveform amplitude converged in a few seconds, the 'bite' was still not fully stable after 15 min CPU time. Further, when the conventional transient was driven by a sine rather than a cosine input the convergence of the 'bite' occurred from opposite directions, i.e. one would initially overestimate the 'bite' and the other would underestimate it. The simulator used in these conventional transient simulations was an in-house simulator called PSTAR. The long PSTAR runtime is not due to an inefficient solution process. PSTAR itself has been compared to the commercially available circuit simulator SPECTRE [2] and is judged to be equivalent in terms of runtimes.

### 3.2 Varicap tuner circuit

The next circuit analysed was that of the varicap tuner shown in Fig. 4. The varicap diode was modelled by a parallel combination of a nonlinear capacitor and a nonlinear resistor (diode form, eqn. 9). The variable capacitance was fitted by a 12th-order polynomial in voltage and was valid in the range 0–23 V. The coefficients were

$$C_0 = 2.276121 \times 10^{-11} \quad C_1 = -9.940123 \times 10^{-12}$$
$$C_2 = 4.600225 \times 10^{-12} \quad C_3 = -1.602318 \times 10^{-12}$$
$$C_4 = 3.839046 \times 10^{-13} \quad C_5 = -6.311486 \times 10^{-14}$$
$$C_6 = 7.187672 \times 10^{-15} \quad C_7 = -5.700524 \times 10^{-16}$$
$$C_8 = 3.132829 \times 10^{-17} \quad C_9 = -1.168078 \times 10^{-18}$$
$$C_{10} = 2.816101 \times 10^{-20} \quad C_{11} = -3.956508 \times 10^{-22}$$
$$C_{12} = 2.458037 \times 10^{-24}$$

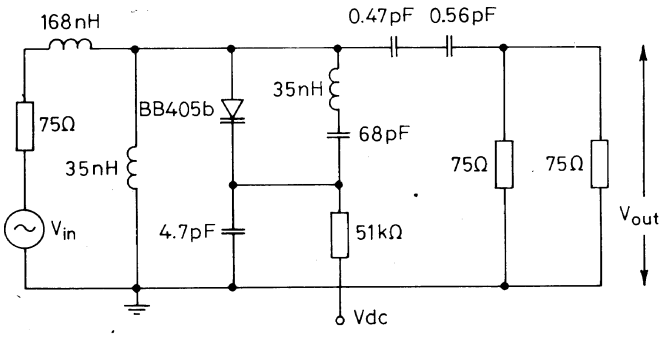


**Fig. 4** *Simulated varicap tuner circuit*

LARGESS was used to simulate the output voltage as a function of frequency and input voltage amplitude at 10 V DC bias; the results are plotted in Fig. 5. Bias

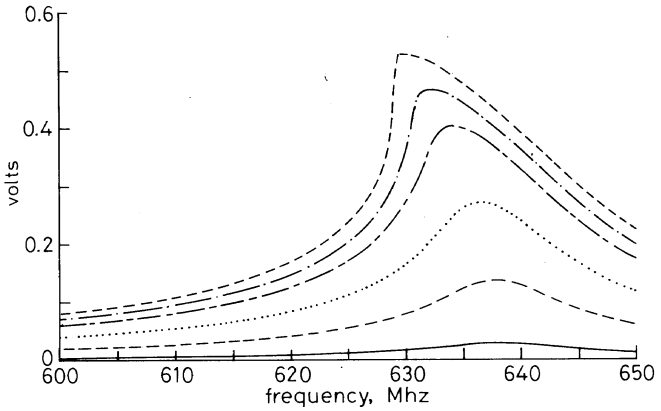


**Fig. 5** *$V_{out}$, at 10 V DC, as a function of frequency and AC input amplitude*
——— 0.10 V AC
------- 0.50 V AC
····· 1.00 V AC
— - — 1.50 V AC
—·—· 1.75 V AC
- - - - 2.00 V AC

points for this figure were computed at 0.5 MHz steps, i.e. 100 per curve. The initial guess for each frequency sweep was the DC solution; subsequent points used the solution at the previous frequency as the starting guess. The shape of the resonance curves depicted in Fig. 5 is seen experimentally and shows the classic form of a jump resonance [3, 4] which develops as the input amplitude increases. Indeed, for the 2 V input curve convergence problems were experienced in the region of 629 MHz, and the plotted curve could only be obtained from two runs, i.e. one starting at 600 MHz and increasing frequency and one starting at 650 MHz and decreasing frequency. Runtimes averaged approximately 3 s per bias point, using 25 timeplanes. Increasing the number of timeplanes to 49 results in approximately a 1 MHz reduction in resonance frequency.

### 3.3 Full wave rectifier circuit

The next example circuit is a full wave rectifier, as shown in Fig. 6. This circuit was chosen for simulation as it was

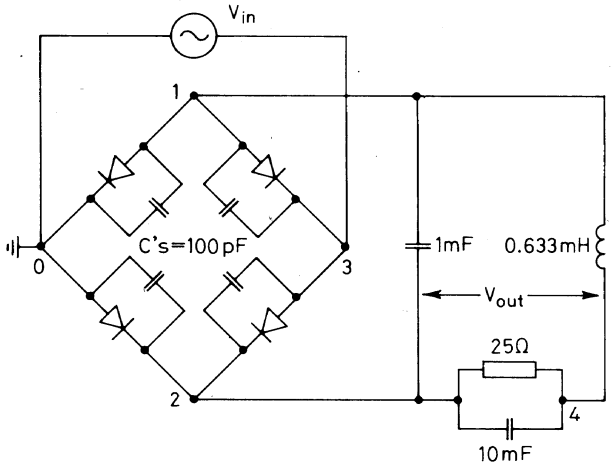


**Fig. 6** *Simulated full wave rectifier circuit*

believed to be a severe test of the accuracy and convergence of the spacetime approach. The diodes in this circuit were modelled purely as nonlinear resistors. Small signal analysis would predict that the only ripple frequencies existing in the output, i.e. the voltage difference between nodes 2 and 4, are at $2n$ times the input frequency, where $n$ is an integer.

In this example the input signal frequency was 50 Hz and two simulation mesh results will be discussed, a 25 Hz mesh spanned by 100 timeplanes and a 50 Hz mesh spanned by 20 timeplanes. The amplitude of any subharmonics could therefore be observed on the 25 Hz mesh, as well as the effect of mesh density on output amplitudes.

Fig. 7 shows how the DC and 100 Hz signal levels are predicted to grow in the output, with increasing input

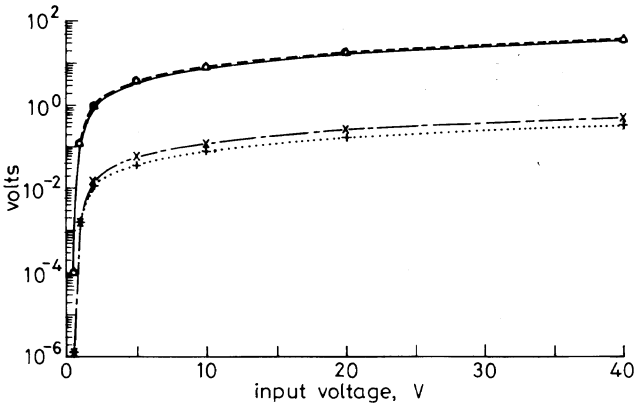


**Fig. 7** *Harmonic amplitudes as a function of input voltage at 50 Hz*

○—○ DC, 25 Hz mesh 100 timeplanes
△--△ DC, 50 Hz mesh 20 time planes
+···+ 100 Hz, 25 Hz mesh 100 timeplanes
×-·-× 100 Hz, 50 Hz mesh 20 timeplanes

amplitude for both meshes. Subharmonics and odd harmonics of the 50 Hz input were all absent, i.e. amplitudes in the numeric noise ($1.0 \times 10^{-14}$ V), and it can be seen that the 20-timeplane mesh yields a solution close to the 25 Hz mesh (50 timeplanes per 50 Hz cycle). Runtimes were approximately 10 s for the 50 Hz 20-timeplane mesh and 500 s for the 25 Hz 100-timeplane mesh.

Additional investigations with mesh densities of 50 and 100 timeplanes per 50 Hz cycle yielded better than 10% agreement between the two meshes up to the 8th harmonic (400 Hz), and within 20% to the 12th harmonic at signal power levels approximately −80 dB down on an input of 40 V (50 Hz), i.e. harmonic signal levels of order $1.0 \times 10^{-3}$ V.

Note that an even number of time planes have been used in these simulations. This was deliberate, as it has been observed that, for odd numbers of timeplanes, subharmonics of the 50 Hz input signal were generated on the 25 Hz mesh that only slowly decayed to zero amplitude with increasing mesh density. Even numbers of timeplanes yielded zero amplitude subharmonics irrespective of the mesh density. This effect is not fully understood and is the subject of further study; it may be related to the chosen first-order discretisation.

## 4 LARGESS simulations: autonomous circuits

Autonomous circuits present two mathematical difficulties to the large signal algorithm. First, and most seriously, as an oscillator runs from a DC supply and is not driven, the phase of any oscillation on the simulation mesh is not uniquely defined. We therefore have an infinity of possible solutions and the resulting system of equations cannot be solved. Secondly, oscillators have unstable DC steady states; in reality noise ensures that these states are not achieved, but in the noiseless world of the circuit model these states need to be actively avoided. Both these difficulties are simultaneously overcome in the following manner.

When attempting to impose a particular phase on an oscillator solution, the first thing to note is that, as we have $n$ equations (current conservation at $n$ spacetime circuit nodes) in $n + 1$ unknowns (the $n$ spacetime nodal voltages and the frequency of oscillation) any method that avoids scanning the frequency must bring in additional equations and possibly unknowns. Therefore, a resistive switched DC voltage source is introduced into the system and arbitrarily connected to one of the circuit nodes. The switch is closed for one timeplane only (at $t = 0$) and is open at all other times. This artifice essentially turns the system into a driven system, which can be solved. To determine the free oscillation of the original oscillator, the potential of the switched voltage source and its switching frequency are adjusted for a zero exchange of energy acrosss the switched link at the only instant in the spacetime-domain when it is closed.

In itself the zero energy transfer condition is not sufficient to uniquely determine the free oscillation, and in addition a requirement of zero differential of the exchange energy with respect to frequency is necessary. The addition of this last condition ensures that if the forcing of a real system is disconnected, the system cannot change frequency, as any such change requires external energy to be supplied.

In the above, note that we have introduced two requirements (equations) i.e.

$$E = \frac{(V_s - V_c)^2 \, \Delta t}{R_s} = 0 \tag{10}$$

and

$$\frac{dE}{df} = 0 \tag{11}$$

where $E$ is the exchange energy, $V_s$ is the forcing voltage of the additional switched DC supply, $V_c$ is the voltage at

the spacetime node to which the switch is connected, $R_s$ is the resistance of the link, $\Delta t$ is the time period for which the switch is closed, and, $f$ is the frequency.

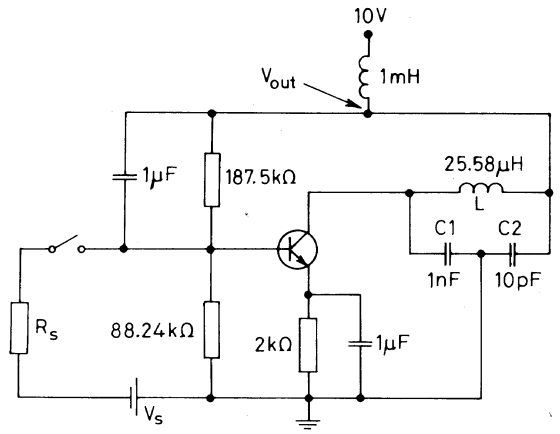


**Fig. 8** *Simulated Colpitts oscillator circuit*

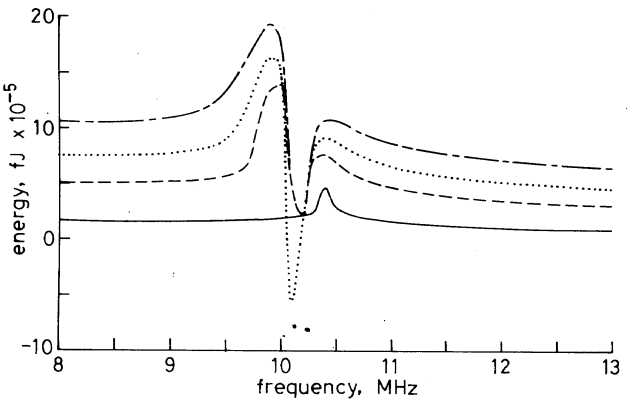


**Fig. 9** *Exchange energy as a function of frequency and forcing voltage*

—— $V_s = 2.70$ V
------- $V_s = 2.60$ V
····· $V_s = 2.55$ V
— - — $V_s = 2.50$ V

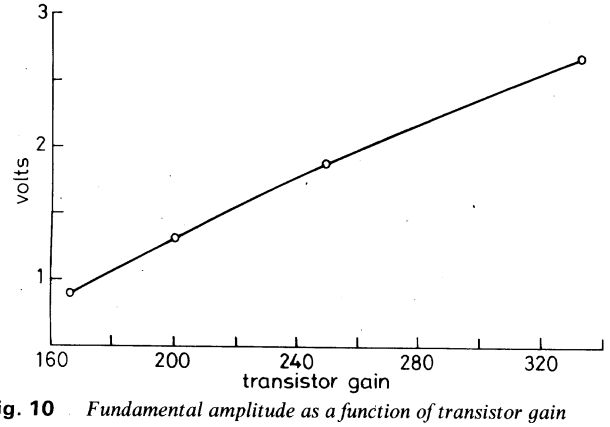


**Fig. 10** *Fundamental amplitude as a function of transistor gain*

We also have an extra unknown in our system — the forcing voltage — and therefore appear to have $n + 2$ equations in $n + 2$ unknowns, i.e. a soluble system. However, when attempting to solve eqn. 11, estimates of the differential of the nodal voltage $V_c$ with frequency are required. Such estimates can be obtained by stepping the frequency toward the required solution, but a direct method can be obtained by solving in parallel two 'copies' of the oscillator at slightly different frequencies $f$ and $f + \Delta f$, where $f$ is a variable, i.e. two spacetime cylinders are used, yielding an overall system of $2n + 2$ equations in $2n + 2$ unknowns, which is directly soluble.

The above forcing process, which can be carried out experimentally, not only imposes the required phase condition on the solution but also avoids the unstable DC steady state by a suitable choice of initial value for the forcing voltage.

The direct method, i.e. solving the $2n + 2$ equations, can in practice only be applied from an initial condition close to the answer. This close initial condition is obtained by frequency-stepping the problem consisting of $n$ current conservation equations in the $n$ unknown nodal potentials while adjusting the forcing voltage after each sweep to obtain a minimum in the exchange energy when plotted against frequency. Once this initial condition is known the procedure for generating the parallel problem is performed by LARGESS automatically, i.e. the user is not aware and does not have to guide the process, apart from an initial specification of a value to be used for $\Delta f/f$.

This algorithm for autonomous circuits will be illustrated by analysing the behaviour of a Colpitts oscillator.

### 4.1 Colpitts oscillator circuit

Fig. 8 shows the circuit to be analysed, in which the transistor was again represented by an Ebers–Moll model as in the amplifier circuit of Fig. 2. Included in Fig. 8 are the switch elements that are used to obtain the solution. These do not form an integral part of the Colpitts oscillator itself.

A small signal analysis of the above circuit yields an oscillation frequency [5] of

$$f_0 = \frac{1}{2\pi}\sqrt{\left(\frac{C_1 + C_2}{LC_1C_2}\right)} = 10 \text{ MHz} \tag{12}$$

provided the transistor gain satisfies

$$\beta \geq \frac{C_1}{C_2} = 100 \tag{13}$$

A small signal analysis cannot yield any information on the amplitude of the oscillation, as this is determined by the nonlinearities in the system. In a real circuit the frequency of oscillation would also depend on the amplitude of oscillation via the transistor junction capacitances. However, the simple Ebers–Moll model used here has no capacitative elements.

The first step in the solution procedure is to scan frequency $f$ while adjusting the value of the forcing voltage $V_s$. Fig. 9 plots the resulting exchange energy for the case where $\beta = 200$, i.e. energy supplied to the oscillator via the link, as a function of $f$ and $V_s$. As $V_s$ is progressively decreased from 2.7 V to 2.5 V (the corresponding DC value of $V_c$ is 2.82966 V) we see the development of a 'volcano'-type energy curve in which a shallow minimum forms. This minimum progressively deepens as the outer 'volcano walls' grow, until the minimum value becomes negative (for $V_s = 2.55$ V). We are searching for the values of $V_s$ and $f$ for which the minimum value is exactly zero.

The method proceeds by loading in a solution from within the minima of one frequency scan that exhibits a negative exchange energy, then creating and solving a parallel problem at a slightly different frequency but the same $V_s$ ($\Delta f/f = 0.001$ in this case). These two problems are then combined and the variables $V_s$ and $f$ added to the system, so that we have $2n$ current conservation equations + eqns. 10 and 11, in $2n + 2$ unknowns, which is then solved, yielding the amplitude and frequency of free oscillation. For this case, where $\beta = 200$, we obtain